Biol. Cell (2012) **104**, 1–18 DOI: 10.1111/boc.201100074

Research article

DOI: 10.1111/boc.201100074

Research article: In this work, we found that moesin interacts with NKCC2 in renal cell lines and in the rat renal medullae. Interestingly, the expression of the dominant negative N-moesin–GFP construct accumulated a NKCC2 construct (c-NKCC2) expressed in LLC-PK1 cells, in intracellular vesicles, suggesting that moesin is required for apical membrane localisation of NKCC2. Our findings suggest a possible involvement of moesin in regulation of Na^+ and Cl^- absorption in the kidney.

Identification of moesin as NKCC2-interacting protein and analysis of its functional role in the NKCC2 apical trafficking

M. Carmosino, F. Rizzo, G. Procino, L. Zolla, A. M. Timperio, D. Basco, C. Barbieri, S. Torretta, M. Svelto

Biol. Cell (2012) **104**, 1–18

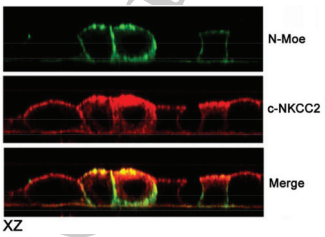

Biol Cell 2012, 104(0), DOI:10.1111/boc.201100074

UNCORRECTED PROOF

Biol. Cell (2012) **104**, 1–18 DOI: 10.1111/boc.201100074

Research article

Identification of moesin as NKCC2-interacting protein and analysis of its functional role in the NKCC2 apical trafficking

Monica Carmosino*†[1], Federica Rizzo*, Giuseppe Procino*, Lello Zolla‡, Anna Maria Timperio‡, Davide Basco*, Claudia Barbieri*, Silvia Torretta* and Maria Svelto*‖

*Department of Biosciences, Biotechnologies and Pharmacological Sciences, University of Bari, 70126 Bari, Italy, †Department of Chemistry, University of Basilicata, Potenza, Italy, ‡Department of Environmental Sciences, Tuscia University, 01100 Viterbo, Italy, and ‖Centro di Eccellenza di Genomica in campo Biomedico ed Agrario, 70126 Bari, Italy

Background information. The renal Na^+–K^+–$2Cl^-$ co-transporter (NKCC2) is expressed in kidney thick ascending limb cells, where it mediates NaCl re-absorption regulating body salt levels and blood pressure.

Results. In this study, we used a well-characterised NKCC2 construct (c-NKCC2) to identify NKCC2-interacting proteins by an antibody shift assay coupled with blue native/SDS-PAGE and mass spectrometry. Among the interacting proteins, we identified moesin, a protein belonging to ezrin, eadixin and moesin family. Co-immunoprecipitation experiments confirmed that c-NKCC2 interacts with the N-terminal domain of moesin in LLC-PK1 cells. Moreover, c-NKCC2 accumulates in intracellular and sub-apical vesicles in cells transfected with a moesin dominant negative GFP-tagged construct. In addition, moesin knock-down by short interfering RNA decreases by about 50% c-NKCC2 surface expression. Specifically, endocytosis and exocytosis assays showed that moesin knock-down does not affect c-NKCC2 internalisation but strongly reduces exocytosis of the co-transporter.

Conclusions. Our data clearly demonstrate that moesin plays a critical role in apical membrane insertion of NKCC2, suggesting a possible involvement of moesin in regulation of Na^+ and Cl^- absorption in the kidney.

Supporting Information available online

UNCORRECTED

Introduction

The renal-specific Na^+–K^+–$2Cl^-$ co-transporter (NKCC2) is expressed exclusively in the mammalian kidney where it provides the major route for sodium/chloride transport across the apical plasma membrane of the thick ascending limb (TAL) cells (Russell, 2000). NKCC2 plays a pivotal role in regulating body salt levels and blood pressure. Indeed, loop diuretics, the pharmacological inhibitors of NKCC2, are among the most powerful antihypertensive drugs available to date (Gamba, 1999). Inactivating mutations of NKCC2-encoding gene have been shown to impair the function and the apical targeting of NKCC2, causing Bartter syndrome type 1, a life-threatening kidney disease (Simon et al., 1996). Recently, other rare missense mutations, associated with clinically reduced blood pressure and protection from hypertension, have been identified (Ji et al., 2008). These mutations result in NKCC2 proteins with impaired transport activity caused by

Monica Carmosino and Federica Rizzo contributed equally to this work.

[1]To whom correspondence should be addressed (email monica.carmosino@uniba.it).

Key words: Kidney, Membrane Transport, Protein sorting/trafficking/targeting.

Abbreviations used: BN/SDS-PAGE, blue native/SDS-PAGE; CBB, Coomassie brilliant blue; ERM, ezrin–radixin—moesin; LLC-PK1, Lilly Laboratories cell porcine kidney; MS, mass spectrometry; MPCs, multi-protein complexes; NKCC2, Na^+–K^+–$2Cl^-$ co-transporter; TAL, thick ascending limb.

© 2012 Soçiété Française des Microscopies and Soçiété de Biologie Cellulaire de France

boc-sgml.cls (2004/08/18 v1.0 LaTeX document class BOC) boc201100074.xml June 28, 2012 21:57

defects in protein processing, trafficking, turnover rate, regulation and ion affinity (Acuna et al., 2011; Monette et al., 2011). Moreover, in spontaneously hypertensive rats (SHRs) during transition from pre-hypertensive state to established hypertension, there was a marked increase in the total expression of NKCC2 and in its distribution to plasma membrane that was not related to increase in levels of NKCC2 mRNA (Sonalker et al., 2004, 2007). This suggested that NKCC2 over-expression was due to a greater translational efficiency or an enhanced stability in SHR. In addition, TAL tubules from Dahl salt-sensitive (DS) rats, a model of salt-dependent hypertension, exhibited significantly higher NKCC2 activity than Dahl salt-resistant strain. Western blot analysis revealed that NKCC2 showed a different pattern of glycosylation in DS rats, suggesting that NKCC2 might accumulate at different stages of its biosynthesis or degradation in these rats (Alvarez-Guerra and Garay, 2002). Recently, it has been observed an increase in NKCC2 surface expression by about 50% in isolated TAL from DS rats under high salt diet without affecting total NKCC2 expression or phosphorylated NKCC2, suggesting that either the hormonal control of NKCC2 trafficking or the intrinsic trafficking mechanisms regulating surface NKCC2 expression are altered in DS rats (Haque et al., 2011). Of note, we recently demonstrated that in the kidney of Milan hypertensive strain (MHS) of rats, the phosphorylation level and the activation state of NKCC2 are strongly up-regulated compared with age matching normotensive control rats, accounting for the genesis and maintenance of the hypertension in MHS rats (Carmosino et al., 2011).

Altogether, these findings highlighted the need to analyse the molecular mechanisms underlying intracellular trafficking and membrane stability of NKCC2 to gain insight into the patho-physiology of salt and water retention. Currently, little is known about NKCC2 regulation in renal cells, mainly because of the difficulty in expressing the co-transporter protein in mammalian cells (Mount, 2006).

To explore factors that regulate NKCC2 sorting and function, we previously generated a chimeric NKCC2 cDNA construct that provides apical expression of NKCC2 when stably transfected in renal epithelial cells (Carmosino et al., 2008) and demonstrated that the interaction between NKCC2 and MAL/VIP17, a protein of the tetraspan membrane proteins family, is involved in stabilisation of the co-transporter into the apical membrane and in its activation (Carmosino et al., 2010).

To look for NKCC2-interacting proteins, we used a proteomic approach based on two-dimensional blue native/SDS-PAGE (BN/SDS-PAGE) coupled with mass spectrometry (MS) in LLC-PK1 cells stably transfected with the chimeric NKCC2 protein. This technique allows to preserve and separate native multi-protein complexes (MPCs) (Schagger and von Jagow, 1991) and to identify those protein–protein interactions occurring under physiological conditions (Camacho-Carvajal et al., 2004). Among the likely binding partners of NKCC2 identified in our study, we focused our attention on radixin and moesin, two members of the ezrin, radixin and moesin (ERM) family of proteins. ERM proteins share a conserved structure including two main functional domains: the N-terminal portion, which binds to protein targets at the plasma membrane, and the C-terminal portion, containing the binding site for F-actin. In the closed (or inactive) conformation, the C-terminus of each ERM protein tightly binds to its own N-terminus domain, thus preventing the interaction with both membrane targets and actin. Upon activation of ERM proteins by phosphatidylinositol 4,5-bisphosphate binding and phosphorylation, this intramolecular interaction is released, and the N-terminal domain is free to bind to its protein targets, whereas the C-terminus binds to actin filaments (Gary and Bretscher, 1995). Regulated attachment of membrane proteins to F-actin is essential for many fundamental processes including the determination of cell shape and surface structure, cell adhesion and motility and integration of membrane transport with signalling pathways. It is not surprising, therefore, that ERM proteins have been implicated in membrane–protein localisation and membrane transport placing them at the crucial juncture in the integration of cortical function.

In this study, we report evidences that moesin is an interacting protein of NKCC2 in epithelial cells and is necessary for the exocytosis and membrane expression of the co-transporter.

UNCORRECTED PROOF

boc-sgml.cls (2004/08/18 v1.0 LaTeX document class BOC) boc201100074.xml June 28, 2012 21:57

Figure 1 | Antibody shift assay

(**A**) Western blotting analysis using T4 antibody of c-NKCC2-transfected LLC-PK1 cell lysates separated by BN-PAGE and blotted on Immobilon P. A single immunoreactive band was detected at about 900 kDa in the lanes loaded with lysate from c-NKCC2-transfected LLC-PK1 cells (lanes 1–2), suggesting that c-NKCC2 formed only one MPC. Incubation of c-NKCC2-transfected cells lysate with T4 antibody caused an upward shift of the band to 1MDa (lane 3). No bands with the same size were visible in all negative controls (lanes 4–6). (**B**) CBB staining of BN-PAGE gel. Asterisk in lane 3 indicated that the band at about 1 MDa corresponding to c-NKCC2 MPC shifted up after incubation with T4 antibody.

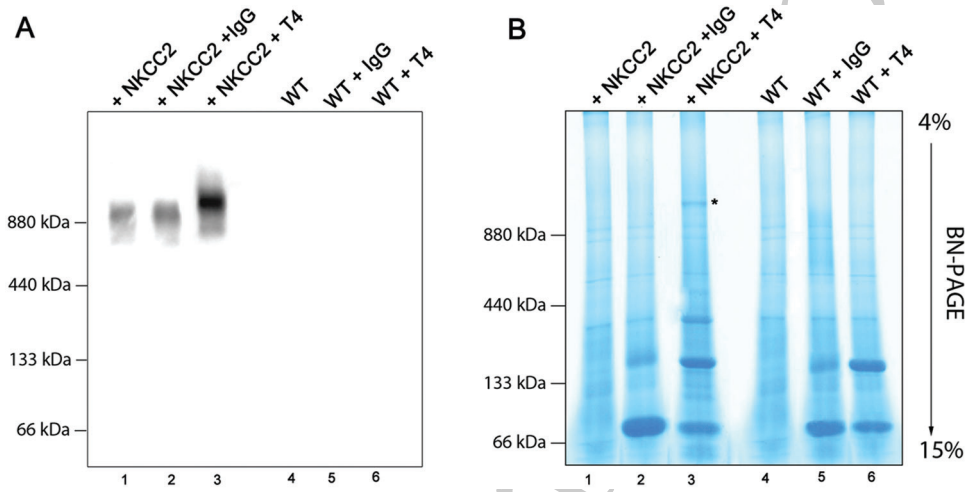

Results

Identification of c-NKCC2-interacting proteins by antibody shift assay

Identification and characterisation of NKCC2-interacting proteins are a pre-requisite for the understanding of NKCC2 regulation mechanisms.

One method for the high-resolution separation of native proteins and MPCs is the antibody shift assay in the BN-PAGE (Liu et al., 2009).

The inclusion of an anti-NKCC2 antibody (T4 antibody) in the lysates from NKCC2 expressing tissues should slow down the electrophoretic mobility of NKCC2/MPCs that can associate with this antibody. Moreover, the choice of non-denaturating conditions of the BN-PAGE preserves both the binding of T4 antibody to NKCC2 and the interaction between the co-transporter and its interacting proteins.

In order to identify NKCC2-interacting proteins, we performed an antibody shift assay on lysates from renal epithelial LLC-PK1 cells stably transfected with a previously characterised NKCC2 construct, c-NKCC2 (Carmosino et al., 2008). Cell lysates were incubated with T4 antibody, and then subjected to a BN-PAGE. Gels were blotted onto PVDF membrane for Western blotting (Figure 1A) or stained with colloidal Coomassie brilliant blue (CBB) (Figure 1B). The experimental conditions include lysates from the following:

(i) c-NKCC2-transfected LLC-PK1 cells (lane 1, + c-NKCC2).
(ii) c-NKCC2-transfected LLC-PK1 cells pre-incubated with an irrelevant IgG (lane 2, + c-NKCC2 + IgG).
(iii) c-NKCC2-transfected LLC-PK1 cells pre-incubated with T4 antibody (lane 3, + c-NKCC2 + T4).
(iv) Untransfected LLC-PK1 cells (lane 4, WT).
(v) Untransfected LLC-PK1 cells pre-incubated with an irrelevant IgG (lane 5, WT + IgG).
(vi) Untransfected LLC-PK1 cells pre-incubated with T4 antibody (lane 6, WT + T4).

Western blotting analysis (Figure 1A) with T4 antibody revealed a single immunoreactive band of about 900 kDa in the lanes loaded with lysates of c-NKCC2-transfected LLC-PK1 cells (lanes 1–2), suggesting that c-NKCC2 formed only one MPC. Interestingly, in the lane loaded with lysate from c-NKCC2-transfected LLC-PK1 cells pre-incubated

UNCORRECTED PROOF

© 2012 Soçiété Française des Microscopies and Soçiété de Biologie Cellulaire de France

boc-sgml.cls (2004/08/18 v1.0 LaTeX document class BOC) boc201100074.xml June 28, 2012 21:57

Table 1 | Summary of trafficking and cytoskeletal proteins identified by MS in the c-NKCC2 MPC

Spot	Mr (kDa)	No. of peptides	Seq Cov (%)	NCBI number	Protein ID
Coat proteins					
2	127,629	4	4	gi|194041120	Co-atomer protein complex, subunit beta 2 (beta prime)
Cytoskeletal proteins					
7	45,162	3	7	gi|45269029	Beta actin
4	68,621	2	3	gi|57527982	Radixin
4	67,733	2	3	gi|57527987	Moesin
Intermediate filament proteins					
6	63,962	2	2	gi|194037336	Cytokeratin 77
12	18,038	2	10	gi|157382506	Cytokeratin 18
3	65,331	5	7	gi|146741296	Cytokeratin 1
Proteasomal proteins					
8	25,703	1	4	gi|1907268	Proteasome activator subunit C9
9	28,668	3	12	gi|47523666	Proteasome activator complex subunit 1
9	24,178	3	14	gi|33317670	Proteasome activator PA28 alpha subunit
10	27,884	1	5	gi|213021241	Proteasome subunit alpha type-6
11	25,864	3	12	gi|222136624	Proteasome subunit beta type-6
Glycosylation enzyme					
5	68,823	1	1	gi|47523726	Dolichyl-diphosphooligosaccharide-protein glycosyltransferase subunit 1
Ribosomal proteins					
13	18,992	4	28	gi|89573899	Ribosomal protein L18
13	17,306	5	26	gi|213983067	60S Ribosomal protein L26
14	15,978	2	18	gi|47523312	40S Ribosomal protein S23
14	14,541	3	23	gi|47523710	60S Ribosomal protein L35
15	13,438	4	19	gi|194018718	40S Ribosomal protein S20

Values are means ± SE of three independent experiments. Student's *t*-test for unpaired data, $^{*}P < 0.005$, $^{**}P < 0.0001$.

with T4 antibody (lane 3), we observed a single band at about 1 MDa, which corresponds to the MPC of c-NKCC2 bound to T4 antibody. The specificity of c-NKCC2 immunoreactive band is demonstrated by the absence of the same immunoreactive band in all the lysates from untransfected LLC-PK1 cells (lanes 4–6). Interestingly, the band immunodetected by the T4 antibody by Western blotting was visualised in a parallel Coomassie-stained BN-PAGE gel (Figure 1B) in c-NKCC2-transfected LLC-PK1 cells pre-incubated with T4 antibody at the expected molecular weight (Figure 1B, lane 3).

To separate the proteins belonging to the c-NKCC2-containing MPC, the identified band was excised from the gel and the single components separated by SDS-PAGE on a 4–15% gradient gel. After the run, the corresponding lane was stained with CBB and 15 single spots were identified. Each spot was excised from the gel and identified by MS that confirmed the presence of c-NKCC2 in the spot # 1, together with (Table 1) several proteins belonging to the trafficking and cytoskeletal categories.

We identified actin, ERM proteins as well as intermediate filaments, all affecting the mobility of intracellular vesicles (spots # 3, 4, 6, 7 and 12). In addition, the MPC contains regulatory elements involved in the protein biosynthetic pathway such as a glycosyltransferase (spot #5) responsible for protein glycosylation in the endoplasmic reticulum (ER) and a subunit of the Golgi Coatomer Complex (spot # 2) essential for Golgi budding and vesicular trafficking. Proteasomal enzymes involved in ATP/ubiquitin-dependent degradation processes in a non-lysosomal pathway have been also identified (spots # 8–11).

The MPC also contains some ribosomal proteins (spots # 13–15), suggesting the presence of a certain amount of c-NKCC2 in the rough ER of LLC-PK1 cells consistent with the possibility that NKCC2, being produced in the ER, has a significant residence time in this organelle.

Among the proteins identified, we focused our attention on the possible role of ERM proteins in NKCC2 trafficking regulation.

UNCORRECTED

Figure 2 | Co-immunoprecipitation of NKCC2 and moesin in LLC-PK1 cells and in rat kidney medullae
(**A**) c-NKCC2 was immunoprecipitated using T4 antibody from LLC-PK1 cells. Western blotting using an anti-moesin monoclonal antibody showed that moesin coimmunoprecipitated with c-NKCC2 (IP, WB moesin). Anti-radixin, anti-ezrin and anti-actin antibodies recognised the cognate bands in cell lysates but not in the immune complexes (WB radixin, WB ezrin and WB actin). (**B**) NKCC2 was immunoprecipitated using T4 antibody from rat kidney outer medullae. Moesin antibody revealed the c-NKCC2 co-immunoprecipitates with moesin (WB moesin). Actin antibody recognised the cognate band in kidney medullae lysates but not in the immune complexes (WB actin). Arrows indicate the T4 antibody IgG.

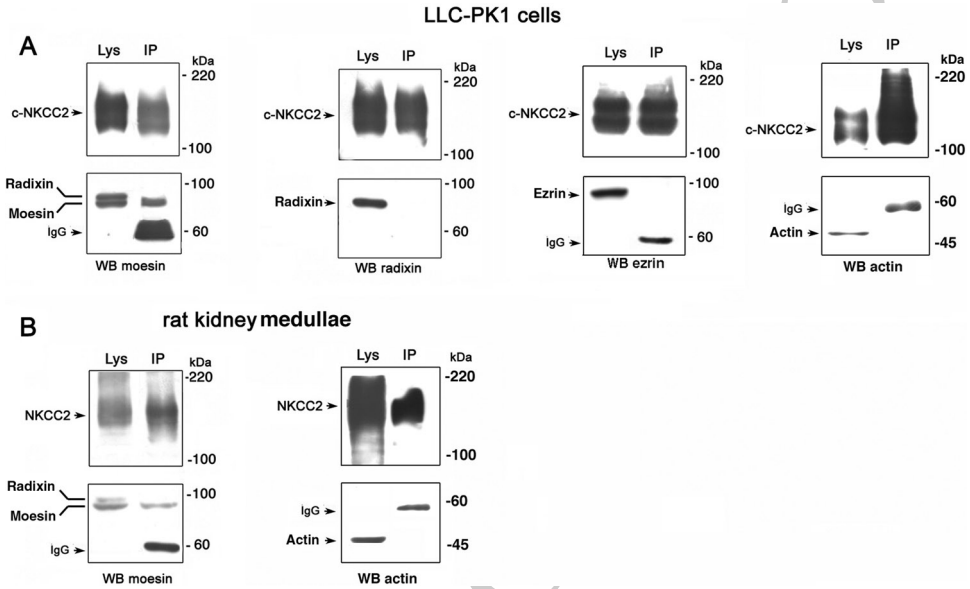

NKCC2 and moesin co-immunoprecipitate and co-localise in LLC-PK1 cells and rat kidney

In the spot # 4, MS analysis identified two peptides corresponding to conserved regions of moesin and radixin, two members of the ERM family of proteins, both involved in regulating the apical trafficking of several transporters. To verify whether NKCC2 interacts with moesin, radixin or both, we carried out co-immunoprecipitation (co-IP) experiments in c-NKCC2 LLC-PK1 expressing cells. Cell lysates were incubated with T4 antibody to immunoprecipitate c-NKCC2 and the resultant immune complexes were resolved by SDS/PAGE and analysed for the presence of moesin and radixin. In cell lysates, the anti-moesin monoclonal antibody, raised against a conserved region of these two ERM proteins, recognised two bands at 78 and 80 kDa, corresponding to moesin and radixin, respectively (Figure 2A, Lys, WB moesin). In the immunoprecipitate, only the lower band corresponding to moesin was revealed, indicating that moesin, but not radixin, interacts with c-NKCC2 (Figure 2A, IP, WB moesin). This indication was further confirmed by the absence of immunoreactive bands in the same immune complexes probed with a specific antibody against radixin (Figure 2A, IP, WB radixin). Although we did not find ezrin in the MS analysis, we verified whether ezrin was an interacting protein of NKCC2. We are able to detect ezrin in the LLC-PK1 cell lysate but not in the NKCC2 IP (Figure 2A, IP, WB ezrin), thus confirming that, among the ERM proteins, NKCC2 specifically interacts with moesin. Since most transporters bind actin and actin binds moesin, we verified whether c-NKCC2 immunoprecipitates with actin in LLC-PK1 cells and kidneys. Actin was detected in the lysate but not in the c-NKCC2 immunoprecipitate, suggesting that c-NKCC2–moesin interaction is not mediated by actin (Figure 2A, WB actin).

To analyse whether moesin and NKCC2 interact *in vivo* we immunoprecipitated NKCC2 from kidney outer medulla lysates and immunodetected moesin in the immune complexes. The Western blotting

UNCORRECTED PROOF

© 2012 Soçiété Française des Microscopies and Soçiété de Biologie Cellulaire de France

boc-sgml.cls (2004/08/18 v1.0 LaTeX document class BOC) boc201100074.xml June 28, 2012 21:57

Figure 3 | Co-localisation of NKCC2 and moesin in LLC-PK1 cells and rat kidney

(**A**) Co-localisation experiments were performed on c-NKCC2-transfected LLC-PK1 cells using a polyclonal anti-HA antibody to stain c-NKCC2 (green) and a monoclonal anti-moesin antibody (red). The merge showed that c-NKCC2 and moesin co-localised at the apical membrane (yellow). (**B**) Sections of rat kidney were stained for NKCC2 (green) and moesin (red). The image merge showed that NKCC2 co-distributes with moesin at the apical membrane of TAL tubules (yellow, merge).

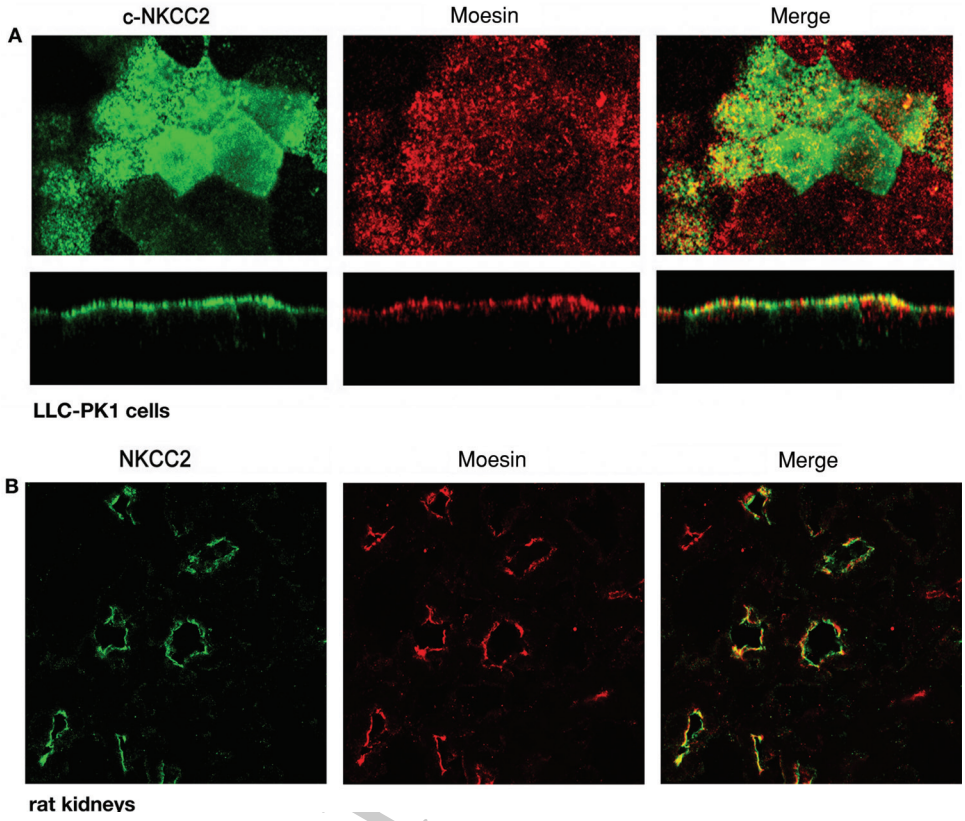

profile of moesin in rat kidney lysates showed the same two bands observed in the LLC-PK1 cells corresponding to radixin (upper band) and moesin (lower band) (Figure 2B, Lys, WB moesin). co-IP experiments showed that NKCC2 selectively interacts with moesin and does not interact with actin in the rat kidney confirming the results obtained in LLC-PK1 cells (Figure 2B, WB moesin, WB actin).

The specificity of the bands found in all co-IP experiments was validated by two negative controls: the co-IP with an irrelevant antibody (rabbit polyclonal anti-rat AQP4 antibody) and a Western blotting of the NKCC2 IP only with the secondary antibody.

We then performed co-localisation experiments in LLC-PK1 cells by immunofluorescence confocal analysis showing that c-NKCC2 and moesin largely co-localised at the apical membrane of LLC-PK1 cells (Figure 3A, merge). To verify whether NKCC2 and moesin co-localise also in the native tissue, we performed co-localisation experiments in rat kidney sections. To label NKCC2, we used the polyclonal R5 antibody, which was specifically raised against the conserved regulatory phospho-threonines in the NKCC N-terminus. The utility of this antibody for immunofluorescence analysis has been well established (Gimenez and Forbush, 2003). Confocal analysis showed that NKCC2 (Figure 3B, green) and moesin (Figure 3B, red) co-localised at the apical membranes of TAL cells (Figure 3B, yellow, merge). Taken together, these findings clearly indicate that moesin is an interacting protein of NKCC2.

UNCORRECTED PROOF

The C-terminal region of NKCC2, containing the apical sorting determinants, is involved in the interaction with the N-terminus of moesin

Given that the C-terminal domain represents the predominant cytoplasmic portion of NKCC2, it is likely to be the region containing the regulatory sites involved in the trafficking of the co-transporter. Indeed, we took advantage of the chimera used in this work and previously described (Carmosino et al., 2008) to verify whether the C-terminal region of NKCC2 is involved in the interaction with moesin. c-NKCC2 is a chimeric protein between NKCC1 and NKCC2 in which we substituted a 150 amino acid stretch of the NKCC2 C-terminal tail, containing the NKCC2 apical sorting determinants, in NKCC1 backbone. To verify whether the interacting region between NKCC2 and moesin sits in the NKCC2 C-terminal region, we performed co-IP experiments in LLC-PK1 cells stably transfected with the secretory basolateral isoform NKCC1 (Figure 4A, LLC-PK1, NKCC1).

In LLC-PK1 cells, we could not detect any moesin immunoreactive band in the NKCC1 immune complexes, likely indicating that moesin preferentially interacts with NKCC2 isoform. However, an alternative explanation for this result is that, even though moesin and NKCC1 could be able to interact, they are expressed in distinct membrane domains in polarised epithelial cells. In fact, in LLC-PK1 cells, NKCC1 is selectively expressed in the basolateral membrane of cells, as previously shown (Carmosino et al., 2010), and moesin in the apical membrane and microvilli (Figure 3A).

Indeed, we performed co-localisation and immunoprecipitation experiments between NKCC1 and moesin in NKCC1 -expressing HEK-293 kidney cells. In this unpolarised cellular model, NKCC1 and moesin co-localise at the plasma membrane (data not shown). Interestingly, even when they are expressed in the same membrane domain, moesin and NKCC1 did not co-immunoprecipitate (Figure 4A, HEK-293, NKCC1), suggesting that the NKCC2–moesin interaction is likely to involve the 150 amino acids stretch of NKCC2 in its C-terminus.

It is possible that moesin-specific binding determinants generated after NKCC1–NKCC2 fusion, thus making the interaction with moesin a specific feature of the chimeric construct.

However, full-length NKCC2 (FL-NKCC2) co-localised and co-immunoprecipitated with moesin in FL-NKCC2 transiently transfected HEK cells, thus confirming that NKCC2 specifically interacts with moesin in cell lines (Figure 4B, HEK293, FL-NKCC2) as well as shown in the native tissue (Figure 2B).

In order to verify whether c-NKCC2 interacts with the N-terminal tail of moesin according to the classical mechanism of interaction of ERM binding proteins (Gary and Bretscher, 1995), c-NKCC2-expressing LLC-PK1 cells were transiently transfected with either N-moesin or C-moesin–GFP-tagged cDNA constructs (Amieva et al., 1999). After the transfection, c-NKCC2 was immunoprecipitated with T4 antibody and the presence of N- or C-moesin constructs in the immunoprecipitates was evaluated using an anti-GFP monoclonal antibody. As shown in Figure 4C, c-NKCC2 co-immunoprecipitated with N-terminal (N-moe–GFP, c-NKCC2) but not with C-terminal moesin construct (C-moe–GFP, c-NKCC2), confirming that c-NKCC2 binds the N-terminal tail of moesin. The molecular weights of N- and C-moesin–GFP constructs were 80 and 62 kDa, respectively, as previously shown (Amieva et al., 1999).

The dominant negative effect of N-moesin construct accumulates c-NKCC2 in intracellular vesicles

It is known that the N-moesin construct acts as a dominant negative element displacing endogenous moesin from both membrane structures and cortical actin. In contrast, C-moesin construct binds to F-actin filaments and lacks the ability to associate with membrane structures without any dominant negative effect on endogenous moesin (Amieva et al., 1999). Indeed, we analysed the effect of the transient expression of N- and C-moesin–GFP constructs on c-NKCC2 trafficking and membrane localisation in LLC-PK1 cells. As shown in Figure 5A, the N-moesin–GFP protein was expressed at the plasma membrane consistent with its ability to compete with endogenous moesin for the membrane protein binding sites (Figure 5A, N-Moe, green signal). Interestingly, the over-expression of N-moesin–GFP accumulated c-NKCC2 in intracellular vesicles (Figure 5A,

UNCORRECTED PROOF

© 2012 Soçiété Française des Microscopies and Soçiété de Biologie Cellulaire de France

boc-sgml.cls (2004/08/18 v1.0 LaTeX document class BOC) boc201100074.xml June 28, 2012 21:57

Figure 4 | Analysis of protein domains involved in the interaction between NKCC2 and moesin

(**A**) LLC-PK1 and HEK-293 cells were transfected with NKCC1 cDNA and subjected to co-immunoprecipitation using T4 antibody. Cell lysates and immune complexes were probed with anti-moesin antibody by WB analysis. Moesin was revealed in cell lysates but not in the NKCC1-containing immune complexes in both cell lines. (**B**) HEK-293 cells were transiently transfected with NKCC2 full-length (FL-NKCC2) and subjected to moesin co-localisation and co-immunoprecipitation assays. Co-localisation experiments showed that moesin (moesin, red) and FL-NKCC2 (FL-NKCC2, green) co-localise at the cell membrane (merge, yellow). WB analysis with anti-moesin antibody revealed the presence of moesin in both FL-NKCC2 cell lysates and immuno complexes. (**C**) c-NKCC2 was immunoprecipitated using T4 antibody from cells transiently transfected with N-moesin–GFP or with C-moesin–GFP constructs. Western blotting analysis using a monoclonal anti-GFP antibody to detect N- or C-moesin showed that c-NKCC2 co-precipitated with N-moesin (N-Moe–GFP) but not with C-moesin (C-Moe-GFP). Arrows indicate the T4 antibody IgG.

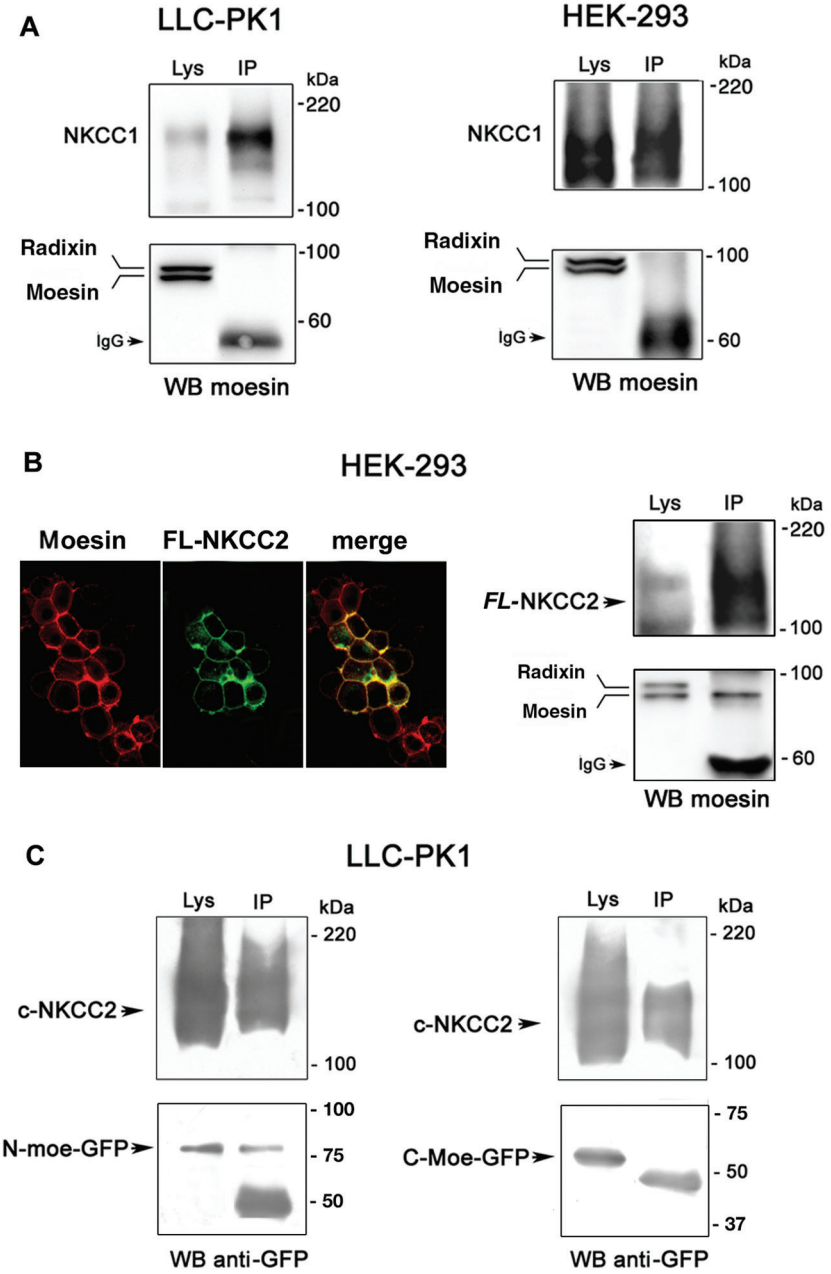

boc-sgml.cls (2004/08/18 v1.0 LaTeX document class BOC) boc201100074.xml June 28, 2012 21:57

Figure 5 | Over-expression of N-Moesin and C-moesin constructs in c-NKCC2-expressing LLC-PK1 cells
(**A**) Cells transiently transfected with N-moesin–GFP (green, N-Moe) or with C-moesin–GFP (green, C-moe) were stained with a polyclonal anti-HA antibody to detect c-NKCC2 (red, c-NKCC2). XZ confocal sections indicated that, in cells expressing N-moesin–GFP, c-NKCC2 accumulated in intracellular and sub-apical vesicles, while in cells expressing C-moesin–GFP, c-NKCC2 was localised at the apical membrane as in C-moesin–GFP negative cells. (**B**) Cells transiently transfected with N-moesin–GFP (green, N-Moe) were stained with a monoclonal anti-Na^+–K^+–ATPase (red, Na^+–K^+–ATPase). XZ confocal sections indicated that Na^+–K^+–ATPase is localised at the basolateral membrane regardless of the expression of N-Moesin–GFP construct (Merge). AQP5–LLC-PK1 cells transiently transfected with N-Moesin–GFP (green, N-Moe) were stained with a polyclonal anti-AQP5 antibody (red, AQP5). XZ confocal sections indicated that AQP5 is localised at the apical membrane regardless of the expression of N-Moe–GFP construct (Merge).

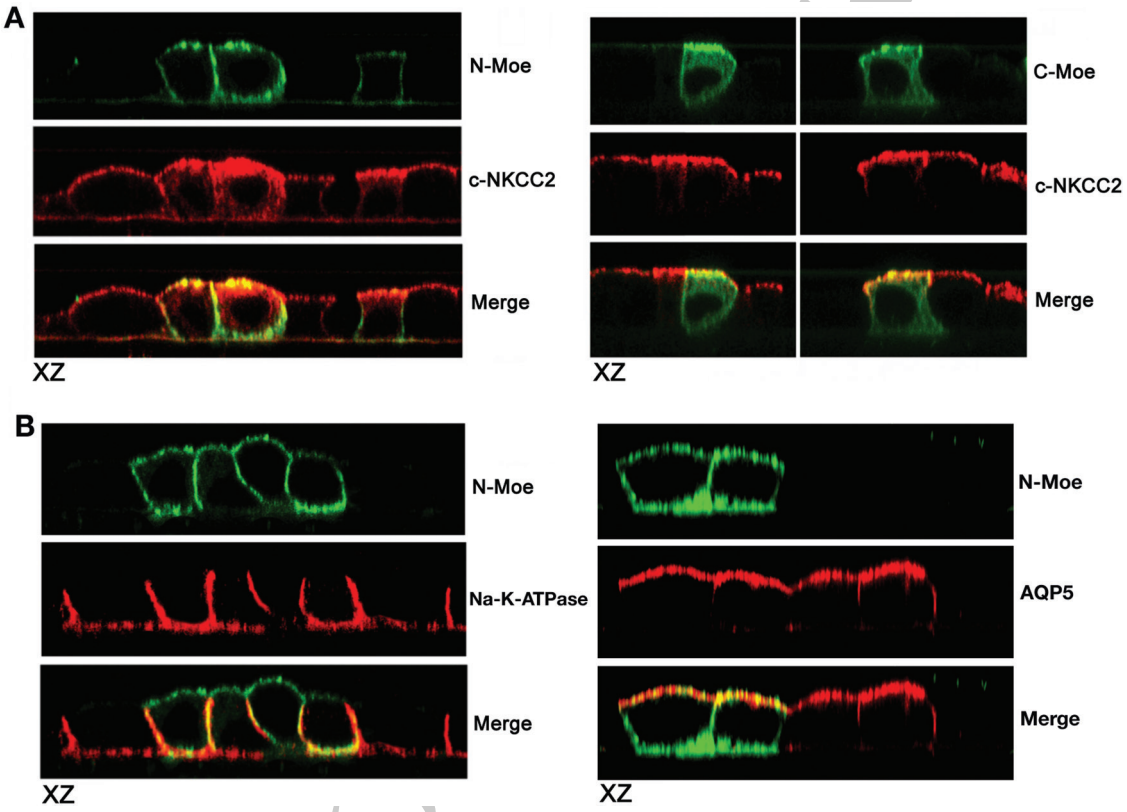

c-NKCC2, red signal). This result suggests that moesin is required for apical membrane localisation of c-NKCC2. In contrast, C-moesin–GFP protein resulted diffusely expressed through the cytoplasm consistent with its ability to bind the actin cytoskeleton (Figure 5A, C-Moe, green signal). In C-moesin–GFP-expressing cells, the membrane localisation of c-NKCC2 was not perturbed compared with control cells (Figure 5A, c-NKCC2, red signal). Taken together, these results indicated that the correct plasma membrane positioning of c-NKCC2 depends on the interaction with moesin and in particular with its N-terminal domain (Figure 5A, c-NKCC2, red).

Since the N-moesin construct is localised along all the plasma membrane in LLC-PK1 cells, we verified whether the trafficking of basolateral proteins, such as the Na–K–ATPase, was impaired in N-moesin-expressing cells. As shown in Figure 5B, the Na–K–ATPase was expressed at the basolateral membrane in both N-moesin positive and negative cells, suggesting that the trafficking of resident basolateral proteins was moesin independent and that the

UNCORRECTED PROOF

© 2012 Soçiété Française des Microscopies and Soçiété de Biologie Cellulaire de France

boc-sgml.cls (2004/08/18 v1.0 LaTeX document class BOC) boc201100074.xml June 28, 2012 21:57

N-moesin-expressing LLC-PK1 cells did not loose their polarisation (Figure 5B, Na–K–ATPase, red).

To verify whether the dominant negative moesin construct was not affecting the overall protein trafficking forward to the apical membrane in LLC-PK1 cells, we analysed the effect of N-moesin construct expression on the apical positioning of anti-aquaporin 5 (AQP5) water channel in LLC-PK1 cells. Similar to NKCC2, AQP5 is localised at the apical membrane of cells in which is expressed and in transfected epithelial cells (He et al., 1997; Ishida et al., 1997; Mhatre et al., 1999; Nielsen et al., 1997; Wellner and Q4 Baum, 2001). Interestingly, we found that AQP5 was expressed at the apical membrane in LLC-PK1 cells transfected with human AQP5, regardless of the pres- Q5 ence of N-moesin construct (Figure 5B, AQP5, red).

Since moesin is involved in several cytoskeleton-mediated cellular processes such as cell motility and polarity, we analyse the effect of the N-moesin construct expression on the cytoskeleton arrangement in LLC-PK1 cells. We found that actin network, visualised by phalloidin–tetramethylrhodamine B isothiocyanate (TRITC), is not perturbed at both apical and basolateral cell sides, by the expression of the dominant negative N-moesin construct, suggesting that the intracellular localisation of c-NKCC2 in this experimental condition is not due to the impairment of the cell cytoskeleton integrity (Supplementary Figure 1).

c-NKCC2 cell surface expression is reduced in moesin-silenced cells

To confirm the role of moesin in the membrane expression of c-NKCC2, we quantified the effect of moesin down-regulation on c-NKCC2 surface localisation by silencing moesin expression in c-NKCC2-transfected LLC-PK1 cells with a specific short interfering RNA (siRNA). We tried different siRNAs against moesin and we selected the most effective one. Western blotting of moesin in lysates prepared from cells treated with scrambled moesin siRNA (mock) and moesin-knock-down cells (moesin KD) confirmed a significant decrease in endogenous moesin in KD cells, by approximately 70% as quantified by the densitometric analysis of moesin band normalised to actin band. In contrast, radixin expression was not affected by moesin siRNA treatment (Figure 6A).

In order to quantitatively evaluate the effect of moesin knock-down on surface expression of c-NKCC2, we performed apical surface biotinylation assay in mock and moesin KD cells (Figure 6B). Apical membrane proteins were biotinylated, using sulfo-N-hydroxysuccinimide (NHS)–SS–biotin, and isolated by precipitation with streptavidin-bound agarose. c-NKCC2 was then identified among the biotinylated proteins by immunoblotting with T4 antibody.

Interestingly, in moesin KD cells, c-NKCC2 surface expression was significantly reduced compared with mock cells (Figure 6B, Biot. c-NKCC2). Importantly, the decrease in NKCC2 surface expression occurred in the absence of a decrease in total cellular amount of c-NKCC2 (Figure 6B, Total c-NKCC2). Densitometric analysis of surface c-NKCC2 normalised to total c-NKCC2 showed a decrease of about 50% in the surface expression of c-NKCC2 in moesin KD cells (Figure 6B, densitometry).

The reduced membrane expression of c-NKCC2 should be paralleled to a decrease in c-NKCC2 activity in LLC-PK1. The NKCCs activation occurs upon the phosphorylation of the membrane expressed NKCC2 at the three conserved threonines in the NKCC N-termini (Darman and Forbush, 2002). Indeed, we followed the phosphorylation dynamics of c-NKCC2 in both mock and moesin KD LLC-PK1 cells by Western blotting using the R5 antibody specifically raised against the NKCC regulatory phosphothreonines.

NKCCs are activated under conditions in which cells are depleted of cytosolic chloride, and we have routinely used low Cl^- pre-incubation to stimulate the chloride transport mediated by NKCCs in mammalian cells (see *Materials and methods*). As shown in Figure 6C, we found that in both steady-state and low chloride conditions, the phopshorylation level of c-NKCC2 was clearly decreased in moesin KD cells compared with mock cells (Figure 6C, Phospho c-NKCC2). Densitometric analysis of Phospho c-NKCC2 normalised to total c-NKCC2 showed a decrease of about 40% in the c-NKCC2 phosphorylation levels in moesin KD cells in all experimental conditions (Figure C densitometry), suggesting a role of moesin also in the regulation of NKCC2 phosphoryaltion. Q6

UNCORRECTED PROOF

boc-sgml.cls (2004/08/18 v1.0 LaTeX document class BOC) boc201100074.xml June 28, 2012 21:57

Figure 6 | Effect of moesin knock-down on c-NKCC2 membrane expression and phosphorylation dynamics in LLC-PK1 cells

(**A**) Endogenous moesin expression was knock-down (KD) with a specific siRNA. Western blotting analysis of cell lysates prepared from control (mock) and moesin KD cells (moesin KD) showed a significant decrease in moesin abundance after siRNA treatment. The densitometric analysis of the moesin bands normalised to actin abundance showed a decrease in 70% of moesin expression in moesin KD cells. Values are means ± SE of three independent experiments. Student's *t*-test for unpaired data, $^{*}P < 0.001$. (**B**) Apical surface biotinylation in mock and moesin KD c-NKCC2-transfected LLC-PK1 cells. Surface proteins were biotinylated and after cell lysis, biotinylated proteins were recovered by precipitation with streptavidin-bound agarose and immunoblotted for c-NKCC2 (Biot. c-NKCC2). The total cellular abundance of c-NKCC2 was evaluated in the lysate of each sample before streptavidin precipitation (Total c-NKCC2). The amount of biotinylated c-NKCC2 was determined from three independent experiments by densitometry of biotinylated c-NKCC2 normalised to total c-NKCC2. Student's *t*-test for unpaired data, $^{*}P < 0.001$. (**C**) Mock and moesin KD c-NKCC2-transfected LLC-PK1 cells were incubated in basic or in low Cl^{-} medium. Cells were then lysed and subjected to Western blotting using R5 antibody. The quantification of phosphorylated c-NKCC2 was determined from three independent experiments by densitometry of phospho-c-NKCC2 bands normalised to total c-NKCC2. Student's *t*-test, $^{*}P < 0.001$.

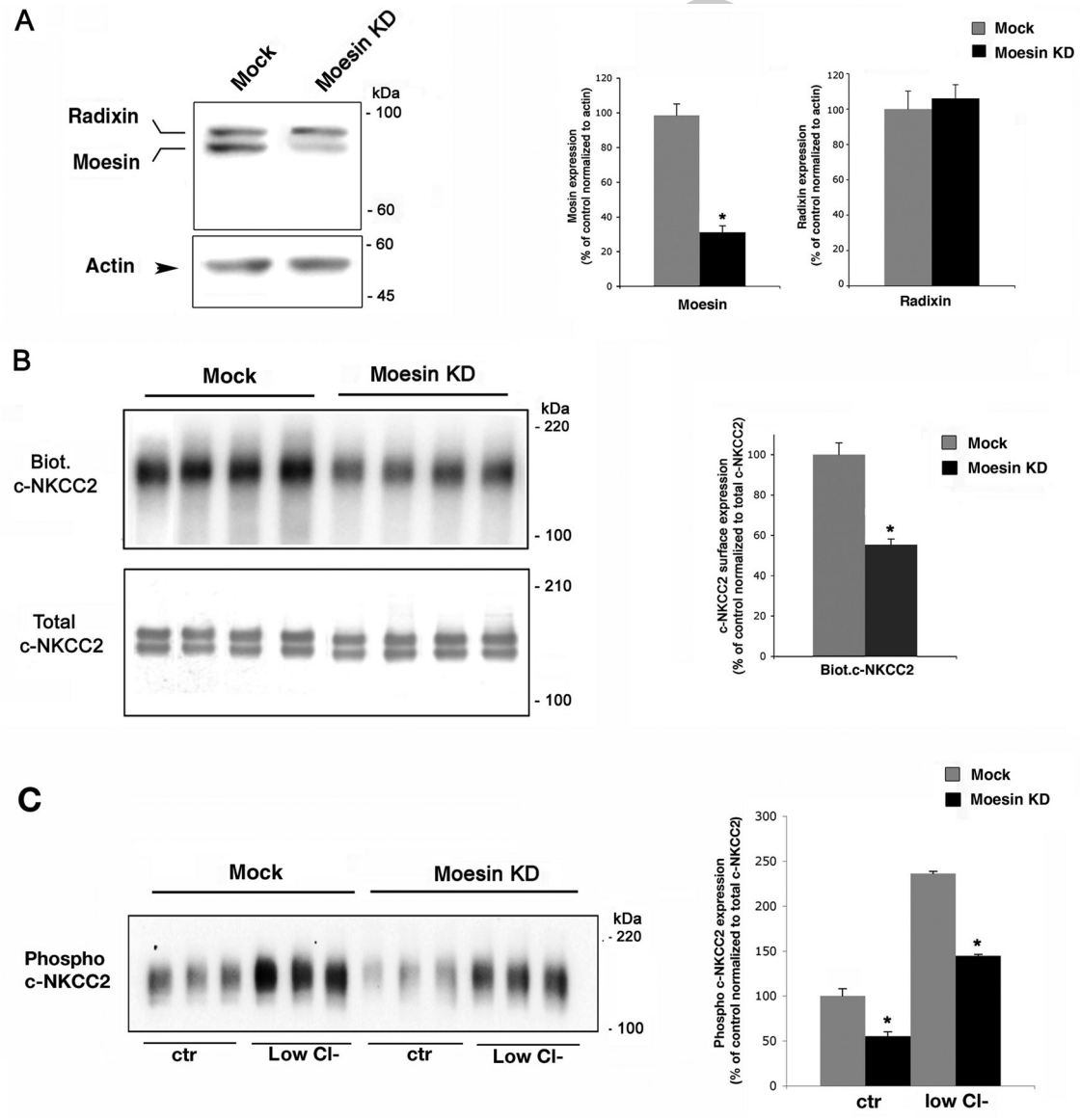

© 2012 Soçiété Française des Microscopies and Soçiété de Biologie Cellulaire de France

boc-sgml.cls (2004/08/18 v1.0 LaTeX document class BOC) boc201100074.xml June 28, 2012 21:57

Figure 7 | Effect of moesin knock-down on both c-NKCC2 endocytosis and exocytosis in LLC-PK1 cells

(**A**) Endocytosis assay. Mock and moesin KD LLC-PK1 cells expressing c-NKCC2 were grown to confluence and biotinylated from the apical side by using a cleavable biotin. Cells were then allowed to internalise surface-labelled proteins for the indicated intervals. The remaining surface accessible biotin was then stripped with MesNa where indicated (MesNa,+). Biotinylated proteins were then recovered with streptavidin-bound agarose, separated by SDS-PAGE and immunoblotted for c-NKCC2. Each experimental condition was performed in triplicate. The amount of internalised c-NKCC2 was calculated by densitometric analysis of biotinylated c-NKCC2 band at 30′ and 60′ of internalisation and visualised as percentage of total cell surface c-NKCC2 (MesNa,−; min. 0). Values are means ± SE of three independent experiments. Student's *t*-test for unpaired data. (**B**) Exocytosis assay. Mock and moesin KD LLC-PK1 cells expressing c-NKCC2 were grown to confluence and pre-treated or not in the presence of membrane-impermeant sulfo-NHS–acetate (NHS–acetate +,−) to quench accessible biotinylable sites. Cells were then biotinylated from the apical side and either maintained at 4°C (NHS–acetate,+; min 0) or returned to 37°C to allow exocytosis for 30′ and 60′. Biotinylated proteins were then recovered by streptavidin–agarose precipitation and immunoblotted for c-NKCC2. Each experimental condition was examined in triplicate. The amount of exocyted c-NKCC2 was determined by densitometric analysis of biotinylated c-NKCC2 bands at 30′ and 60′ of exocytosis and expressed as percentage of total cell surface c-NKCC2 quantified in cells not exposed to sulfo-NHS–acetate (NHS–acetate,−).

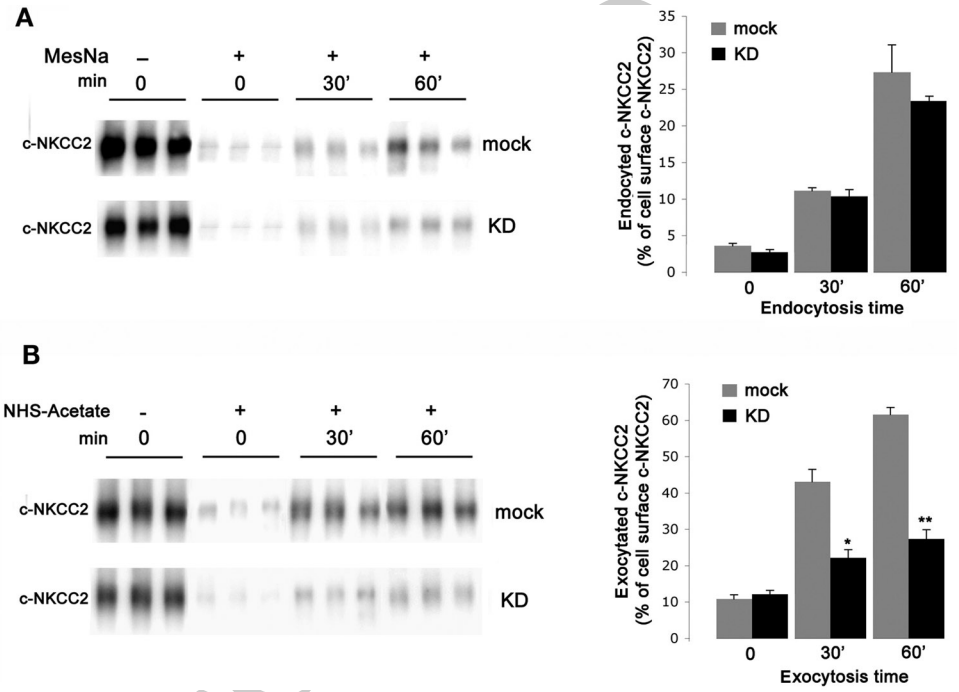

Decreased surface expression of c-NKCC2 in moesin KD cells is due to decreased membrane delivery of c-NKCC2

The reduction in surface expression of c-NKCC2 in moesin KD cells could be attributed to either an increase of c-NKCC2 endocytosis or to a decrease in c-NKCC2 exocytosis to the apical membrane or to both phenomena.

To discriminate between these possibilities, we performed endocytosis and exocytosis assays in mock and moesin KD cells as described in the *Materials and methods* section. The amount of biotinylated c-NKCC2 internalised within 30 and 60 min of observation, normalised to cell surface biotinylated c-NKCC2 at time 0, was not statistically different between moesin KD cells and control cells (mock), indicating that endocytosis was not significantly affected by moesin knock-down (Figure 7A).

On the other hand, we observed that in moesin KD cells, the amount of c-NKCC2 delivered at the apical membrane was significantly decreased at both 30 and 60 min time points by about 40 and 60%,

boc-sgml.cls (2004/08/18 v1.0 LaTeX document class BOC) boc201100074.xml June 28, 2012 21:57

respectively, suggesting a role of moesin rather in c-NKCC2 exocytosis (Figure 7B). However, moesin could be involved either in the Golgi exit of c-NKCC2 along its biosynthetic pathway or alternatively in the c-NKCC2 recycling toward the apical membrane. We found that moesin is not involved in the exit of NKCC2 from the Golgi apparatus since co-localisation experiments of c-NKCC2 with the Golgi marker TGN46 in N-moesin–GFP LLC-PK1 expressing cells showed that NKCC2-expressing vesicles in N-moesin–GFP positive cells were excluded from Golgi area. This demonstrates that the displacement of the endogenous moesin does not affect the exit of c-NKCC2 from the Golgi apparatus (Supplementary Figure 2) and rather suggests that moesin most likely is involved in c-NKCC2 apical recycling.

Discussion

NKCC2 surface expression is subject to regulation by intracellular protein trafficking (Caceres et al., 2009; Gimenez and Forbush, 2003; Ortiz, 2006). However, very little is known about the protein-binding partners that control membrane sorting and stability of NKCC2. Accordingly, identifying proteins that interact with NKCC2 should help to further determine the mechanisms of regulated NKCC2 trafficking.

In this report, we describe a novel proteomic approach based on antibody shift assay coupled with BN/SDS-PAGE and MS to identify possible NKCC2-interacting proteins.

To this end, we used a renal cell line stably transfected with a c-NKCC2 in which the apical sorting determinants of NKCC2 have been exchanged in NKCC1 backbone (Carmosino et al., 2008). Unfortunately, the stable expression of the FL-NKCC2 in epithelial cells resulted so far unsuccessful. It is believed that this is due to the presence of the N-terminal tail of NKCC2. We encountered several problems in the interpretation of the antibody shift assay results and in the evaluation of the polarised trafficking of NKCC2 using LLC-PK1 transiently transfected with the FL-NKCC2. In contrast, the chimeric NKCC2 construct used in this work is stably expressed at the apical membrane and it is functionally active, providing a useful tool for studying the regulation of NKCC2 apical expression in an epithelial cell system. The use of non-denaturing conditions is the main advantage of this experimental approach because it preserves the native form of protein–protein complexes, thus allowing an analysis of the interactions in a physiological condition (Pyndiah et al., 2007).

Recent studies performed with the yeast two-hybrid system identified Aldolase (Benziane et al., 2007) and the Secretory Carrier Membrane Protein 2 (SCAMP2) (Zaarour et al., 2011) as interacting proteins of NKCC2. Both proteins interact with C-terminus of NKCC2 and are involved in the surface expression of the co-transporter. However, the major disadvantages of yeast two-hybrid are that the proteins of interest are expressed in a heterologous system, the yeast, where some post-translational modifications do not, or inappropriately, occur and that the protein–protein interactions are analysed in the nucleus.

Among the proteins identified in the c-NKCC2 MPC, we focused our attention on moesin, since ERM proteins play a crucial role in the regulation of several ion transporters (Levi, 2003).

We confirmed the interaction between c-NKCC2 and moesin by co-IP experiments in stably transfected LLC-PK1 cells.

Of note, we showed that NKCC2 and moesin co-localise and co-immunoprecipitate also in the native tissue, demonstrating that both the NKCC2 chimeric construct and the cellular model used in this work recapitulate the physiological environment in which the NKCC2–moesin interaction occurs.

Moreover, we found that the FL-NKCC2 co-localises and co-immunoprecipitates with moesin in HEK cells, further demonstrating that the interaction with moesin is a specific feature of the native NKCC2. Interestingly, we found that NKCC2 neither interact with other members of ERM family proteins nor with actin, thus suggesting that the NKCC2–moesin interaction is specific and independent of actin. The presence of actin in the MS analysis most likely is due to an unspecific inclusion of this abundant cell protein in the c-NKCC2 MPC.

We found that in cells expressing a GFP-tagged dominant negative N-moesin construct, c-NKCC2 accumulates in intracellular vesicles, suggesting the involvement of endogenous moesin in regulating the membrane localisation of c-NKCC2. Of note, the localisation of the apical protein AQP5 and the basolateral protein Na–K–ATPase as well as the

UNCORRECTED PROOF

© 2012 Soçiété Française des Microscopies and Soçiété de Biologie Cellulaire de France

boc-sgml.cls (2004/08/18 v1.0 LaTeX document class BOC) boc201100074.xml June 28, 2012 21:57

cytoskeleton architecture were not affected by the expression of the N-moesin construct, underlining that the overall apical trafficking and the cell polarity were not altered in this experimental condition. In addition, endocytosis and exocytosis assays showed that moesin knock-down profoundly impaired c-NKCC2 exocytic insertion but did not affect its internalisation. Accordingly, the phosphorylation level of c-NKCC2 in moesin KD cells is significantly lower that in mock cells, suggesting the involvement of moesin in the regulation of NKCC2 phosphorylation dynamics. Most likely, the decrease in phosphorylation level of c-NKCC2 in moesin KD cells is paralleled by a decrease in c-NKCC2 transport rate. However, functional experiments will be necessary to definitively address this issue.

The finding that moesin plays a positive role in c-NKCC2 exocytosis is in agreement with previous observations about the role of ERM proteins in the apical localisation and function of other transmembrane proteins. For instance, NHE3 (Shenolikar and Weinman, 2001), NaPi IIa (Murer et al., 2003) and CFTR (Wang et al., 2000) were found to be associated directly or indirectly with members of ERM family. NHE3 binds ezrin directly or by association with Q7 NHERF-1. The functional role of direct interaction between NHE3 and ezrin is related to the exocytic trafficking and plasma membrane delivery of newly synthesised NHE3, which determines its amount of plasma membrane and, partially, determines its activity (Cha et al., 2006). The binding between NHERF-1 and NaPi IIa is important for the apical sorting/positioning of the co-transporter (Murer et al., 2003). The interaction between NHERF, ezrin and PKA is been hypothesised to be essential to regulate CFTR activity but also to anchor CFTR to the actin cytoskeleton (Short et al., 1998), to stabilise CFTR protein at the apical cell surface (Swiatecka-Urban et al., 2002) and to increase the efficiency by which kinases and phosphatases control channel ac- Q8 tivity (Sun et al., 2000; Liedtke et al., 2002).

Interestingly, it has been observed that ezrin interacts with 1β-adrenergic receptor (AR) and that ezrin knock-down impaired 1β-AR recycling to the plasma membrane without affecting both receptor biosynthesis and internalisation (Stanasila et al., 2006). Altogether, these data indicate that ERM proteins can regulate the protein membrane expression by modulating either the biosynthetic or recycling pathway. Although we have evidences that c-NKCC2 does not accumulate in the Golgi apparatus in dominant negative N-moesin-expressing cells, thus suggesting that moesin is not involved in the biosynthetic pathway of NKCC2, further experiments are necessary to definitively address in which step of the NKCC2 exocytosis process moesin is involved.

In all the examples mentioned above, the interaction with ERM proteins involves the transporters C-terminal tail. Taking advantage of the chimera used in this work, we have been able to narrow the region of interaction with moesin in a 150 amino acidic stretch of NKCC2 C-terminal tail, suggesting that like CFTR, NaPi IIa and NHE3, NKCC2 surface expression depends upon direct or indirect ERM interactions involving the C-terminus.

A recent study demonstrated that surface abundance of NKCC2 in rat TALs at steady state depends upon the balance between constitutive endocytosis and exocytosis (Ares and Ortiz, 2010), indicating that the dynamic trafficking of NKCC2 occurs under baseline conditions in the absence of stimuli. Interestingly, the same authors found that cholesterol depletion completely blocked NKCC2 endocytosis, enhanced surface NKCC2 and net Cl^- transport by TALs, indicating that constitutive trafficking of NKCC2 is essential for re-absorptive function of the TAL (Ares and Ortiz, 2010).

In this context, our results are of particular interest because we identified moesin as a new player regulating c-NKCC2 exocytic insertion in the steady-state conditions.

Although ERM proteins are approximately 70% identical in sequence, structurally similar, and considered functionally equivalent, they have a specific tissue distribution (Bretscher et al., 2002). In the kidney, moesin, together with radixin, is expressed in mesangial and glomerular endothelial cells likely involved in the cell migration and glomerular remodelling (Hugo et al., 1996). In addition, moesin has been shown to be specifically expressed in the outer medulla (Kraemer et al., 2003), precisely in TAL cells (Dihazi et al., 2005), and to be absent in inner medulla collecting ducts (Uawithya et al., 2008), underlining the physiological relevance of our findings.

Two prominent characteristics of epithelial cells, apical–basal polarity and a highly ordered cytoskeleton, depend on the existence of precisely localised

UNCORRECTED PROOF

boc-sgml.cls (2004/08/18 v1.0 LaTeX document class BOC) boc201100074.xml June 28, 2012 21:57

protein complexes associated with the apical plasma membrane and on a separate machinery that regulates the spatial order of actin assembly. Moesin links transmembrane proteins to the actin cytoskeleton in the apical domain, suggesting a crucial role in epithelial cell polarity and in signalling pathways. Indeed, we suggest that the involvement of moesin in the precise localisation of NKCC2 at the apical membrane of TAL cells contributes both to the apical–basal polarity of these renal epithelial cells and to the regulation of Na^+ and Cl^- re-absorption in the kidney.

In this study, we also identified other proteins contained into c-NKCC2 MPC likely involved either in trafficking or degradation of the co-transporter (Table 1).

Of note, we found proteasome subunits in the c-NKCC2 MPC, suggesting that they could be the NKCC2-interacting components responsible for the degradation of NKCC2 Bartter mutants. In fact, several NKCC2 Bartter mutants showed a low expression level when expressed in Oocytes, suggesting that they are subjected to early degradation by the ER cellular quality control system involving activation of ubiquitin–proteasome proteolitic pathway (Starremans et al., 2003).

We cannot exclude that these interacting proteins, identified by the use of chimera, are NKCC1 rather than NKCC2 molecular partners. Indeed, as performed for moesin, further experiments will be necessary to verify whether they are actually binding partners of NKCC2 and in this case to analyse their possible role in the NKCC2 regulation.

Materials and methods

Constructs and antibodies

The chimeric c-NKCC2 and the FL-NKCC2 used in this work correspond to the previously described chimera IV–VI and NKCC2, respectively (Carmosino et al., 2008). N- and C-moesin–GFP constructs were kindly provided by Dr Francisco Sanchez-Madrid (Servicio de Immunología, Hospital Universitario de La Princesa, Madrid, Spain) and previously characterised (Amieva et al., 1999). The monoclonal T4 antibody was from Developmental Studies Hybridoma Bank, the University of Iowa, IA, USA. The monoclonal anti-moesin and anti-ezrin antibodies, the rabbit polyclonal anti-radixin, the rabbit polyclonal anti-HA and the monoclonal anti-HA antibodies were from Sigma–Aldrich. The monoclonal anti-GFP antibody was from Covance. The goat polyclonal anti-actin and AQP5 antibodies were from Santa Cruz Biotechnology. The monoclonal anti-Na^+/K^+ ATPase antibody was from Upstate. The rabbit polyclonal anti-phosphorylated NKCC, R5 antibody was generated and characterised by Prof Biff Forbush (Yale University, New Haven, CT, USA). The rabbit polyclonal anti-TGN46 antibody was from Abcam.

Cell culture, transfection and animals

LLC-PK1 and HEK cells were maintained in DMEM, 2 mM L-glutamine, 10% fetal bovine serum, penicillin (50 U/ml) and streptomycin (50 U/ml) at 37°C, 5% CO_2 in a humidified incubator. For transfection, cells were grown until approximately 95% confluent and then transfected with HA-tagged c-NKCC2, with HA-tagged NKCC1, HA-tagged NKCC2 or human AQP5. Lipofectamine 2000 (Invitrogen) was used for transfection according to the manufacturer's instructions. Stable clones were selected in culture medium supplemented with 1 mg/ml geneticin.

Kidneys of Wistar–Kyoto rats (from Harlan) were used for co-IP and co-localisation experiments.

Antibody shift assay

LLC-PK1 cells wild type or transfected with c-NKCC2 were washed in ice-cold PBS-CM and scraped in ice-cold BN lysis buffer (500 mM ε-aminocaproic acid, 20 mM Bis–Tris, 2 mM EDTA, 12 mM NaCl, 10% glycerol pH 7 with 0.5% Triton X-100). The lysis was performed on ice for 1 h and the samples were then centrifuged at 22,000*g* for 30 min at 4°C. The protein content of the supernatant was measured with BCA Protein Assay Kit (BioRad).

Three hundred micrograms of cellular protein extracts were combined with 3 μg of T4 antibody and incubated on ice for 30 min before loading the mixture on the BN-PAGE. An equivalent amount of cellular protein lysates was combined with 3 μg of an irrespective antibody used as a negative control. BN-PAGE was performed according to Basco et al. (2010). Briefly, for first dimension, the samples were added to BN sample buffer (750 mM ε-aminocaproic acid and 5% CBB G-250) and loaded onto the gel. Electrophoresis was performed at 10 mA and stopped when the tracking line of CBB G-250 dye had left the edge of the gel. The gel was stained with colloidal CBB G-250 overnight or blotted onto an Immobilon P membrane (Millipore) for Western blot analysis with T4 antibody to detect c-NKCC2.

The shifted-up protein complex band was then cut out from the Coomassie-stained gel, equilibrated in denaturing buffer (1% SDS and 1% β-mercaptoethanol) for 30 min at room temperature (RT) and successively placed on top of a 4–15% SDS-PAGE gel. At the end of the run, the gel was stained with colloidal CBB G-250 overnight.

In-gel digestion and protein identification by nano-RP-HPLC–ESI–MS/MS

MS procedures were performed as previously described (Basco et al., 2011). Q9

co-IP experiments

c-NKCC2-, NKCC1- or FL-NKCC2-expressing cells were washed in ice-cold PBS-CM and scraped in lysis buffer (150 mM NaCl, 30 mM NaF, 5 mM EDTA, 15 mM Na2HPO4, 15 mM pyrophosphate and 20 mM HEPES, pH 7.2 with 0.5% Triton

UNCORRECTED PROOF

© 2012 Soçiété Française des Microscopies and Soçiété de Biologie Cellulaire de France

boc-sgml.cls (2004/08/18 v1.0 LaTeX document class BOC) boc201100074.xml June 28, 2012 21:57

X-100). After 1 h of lysis on ice, lysates were clarified by centrifugation at 13,000*g* for 30 min at 4°C, supernatants were precleared with 100 μl of protein A–sepharose suspension (Sigma–Aldrich) for 1 h at 4°C under rotation and then incubated with 5 μg of monoclonal antibody T4 overnight at 4°C under rotation to immunoprecipitate NKCC. Immune complexes were isolated using 100 μl of protein A–sepharose suspension for 2 h at 4°C under rotation and then washed five times with lysis buffer. Immune complexes were dissociated in Laemmli buffer with 100 mM DTT, heated at 95°C for 10 min and resolved on gradient 4–15% SDS-PAGE. After transfer to Immobilon P membrane, lanes were probed with antibodies against NKCC (T4 1:1000), moesin (1:1000), radixin (1:500), ezrin (1:1000) and actin (1:500). In experiments in LLC-PK1 cells transfected transiently with constructs for N-moesin–GFP and C-moesin–GFP, lanes were probed with monoclonal antibody anti-GFP (1:1000).

Outer medullae excised from rat kidneys were homogenised in lysis buffer at 25,000 rpm with a Polytron tissue homogeniser (Brinkmann Instruments) and centrifuged at 13,000*g* for 30 min at 4°C. Supernatants were pre-cleared with protein A–Sepharose suspension and then incubated with the T4 antibody overnight at 4°C under rotation to immunoprecipitate NKCC2. Immune complexes were bound to protein A–Sepharose suspension, washed, dissociated in Laemmli buffer and resolved by SDS-PAGE. After protein blotting, the membrane was incubated with antibodies against NKCC2 (T4, 1:1000) and moesin (1:1000) and actin (1:500).

Moesin silencing in LLC-PK1 cells

A Stealth® siRNA from Invitrogen targeting pig moesin was used in combination with Lipofectamine 2000 reagent to knock-down moesin expression in LLC-PK1 cells. The relative amounts of siRNA and Lipofectamine 2000 used in each experiment were decided according to number of plated cells and to the guidelines provided from Invitrogen. When confluent at 70%, c-NKCC2 LLC-PK1 expressing cells were treated with either scrambled moesin siRNA (mock) or moesin siRNA (moesin KD).

To analyse moesin knock-down, after 48 h from the siRNA injection, either mock and moesin KD cells were lysed in lysis buffer with 1% Triton X-100. Lysates were sonicated and then clarified by centrifugation at 13,000*g* for 30 min at 4°C. Equal amounts of total protein were loaded on gradient 4–15% SDS-PAGE and after transfer to Immobilon P membrane, lanes were probed with antibodies against moesin (1:1000) and actin (1:500).

Immunofluorescence

c-NKCC2 LLC-PK1 transfected cells, grown on 0.4 μm cell culture inserts, were fixed in methanol for 5 min. After three washes in PBS, cells were blocked in saturation buffer (1% bovine serum albumin in PBS) for 20 min at RT and incubated with the primary antibodies for 2 h at RT in saturation buffer. After three washes in PBS, cells were incubated with the appropriate Alexa fluor-conjugated secondary antibodies for 1 h at RT. Primary antibodies used were as follows: polyclonal or monoclonal anti-HA antibody (1:1000) to detect c-NKCC2, the monoclonal anti-moesin antibody (1:500), the polyclonal anti-AQP5 antibody (1:500), the monoclonal anti-Na^+/K^+ATPase antibody (1:500) and the polyclonal anti-TGN46 antibody (1:200). Phalloidin–TRITC from Sigma–Aldrich was used to identify filamentous actin.

Kidneys from rats were fixed in paraformaldehyde 4% in PBS and than cryoprotected by incubation overnight in sucrose 30% in PBS. Sections of 5 μm were cut and mounted on Superfrost Plus glass. Immunofluorescence experiments were performed as described above. The primary antibodies used were as follows: rabbit polyclonal R5 antibody (1:1000) to detect NKCC2 and monoclonal anti-moesin antibody (1:500). Confocal images were obtained with a laser scanning fluorescence microscope Leica TSC-SP2 (HCX PL APO, ×63/1.32–0.60 oil objective); 8-bit images were saved at 1024 × 256 and acquired using the Leica Confocal Software.

Apical surface biotinylation

Forty eight hours after transfection with scrambled moesin siRNA, or moesin siRNA, cells were rapidly washed twice in ice-cold EBS buffer for biotinylation (10 mM triethanolamine pH 9.0, 150 mM NaCl, 1 mM MgCl2, 0.1 mM CaCl2) and then incubated with 1.5 mg/ml of Biotin 3-sulfo-NHS ester sodium salt (Sigma–Aldrich) in EBS buffer on ice for 45 min. Cells were washed twice in ice-cold PBS-CM and unbound biotin was quenched twice for 10 min in quenching buffer (50 mM NH_4Cl in PBS-CM) on ice. Cells were scraped in 500 μl of lysis buffer (20 mM Tris–HCl pH 8.0, 150 mM NaCl, 5 mM EDTA, 1% Triton X-100, 0.2% BSA, 1 mM PMSF, protease inhibitors cocktail), lysates were sonicated and incubated at 37°C for 20 min. Insoluble material was pelleted at 13,000*g* for 10 min and biotinylated proteins in the supernatants were precipitated overnight with 50 μl of Immunopure-immobilised streptavidin beads suspension (Pierce) under rotation at 4°C. Beads from each condition were washed three times in lysis buffer. Biotinylated proteins were extracted in 30 μl of Laemmli buffer with 100 mM DTT, heated at 95°C for 10 min and resolved on gradient 4–15% SDS-PAGE. After transfer, Immobilon P membrane was incubated with T4 antibody to detect c-NKCC2.

Activation assay

Mock and moesin KD cells were pre-incubated for 30 min in basic medium (135 mM NaCl, 1 mM $MgCl_2$, 1 mM Na_2SO_4, 1 mM $CaCl_2$ and 15 mM Na–HEPES, pH 7,4) and then they were incubated for 30 min in low Cl^- medium (1 mM NaCl, 1 mM $MgCl_2$, 1 mM Na_2SO4, 1 mM $CaCl_2$, 15 mM Na–HEPES and 134 mM Na gluconate, pH 7.4). After the incubation, cells were scraped in lysis buffer with 1% Triton and 0.5 μM protein phosphatase-1 inhibitor calyculin A (Sigma–Aldrich). Lysates were sonicated and then clarified by centrifugation at 13,000*g* for 30 min at 4°C. Equal amounts of total protein were loaded on gradient 4–15% SDS-PAGE and after transfer to Immobilon P membrane, lanes were probed with antibody against phosphorylated NKCC2 (R5, 1:1000).

Endocytosis and exocytosis assays

Endocytosis assays were performed as previously described (Carmosino et al., 2010). Briefly, cells grown to confluence were biotinylated with cell-impermeable NHS–SS–biotin (Pierce) from the apical side. Cells were returned to 37°C, to permit internalisation of surface proteins, for 30 or 60 min. Next, cells

UNCORRECTED PROOF

boc-sgml.cls (2004/08/18 v1.0 LaTeX document class BOC) boc201100074.xml June 28, 2012 21:57

were treated with the cell-impermeable MesNa that removes cell surface-bound biotin, whereas internalised biotinylated proteins are protected. Cells were lysed and biotinylated proteins were recovered with streptavidin beads suspension under rotation at 4°C overnight.

The exocytosis assay was performed as follows: confluent c-NKCC2-expressing LLC-PK1 cells were washed with PBS-CM and then exposed to 2 mg/ml sulfo-NHS–acetate (Pierce) in PBS-CM for 2 h to saturate NHS-reactive sites on the cell surface as previously described (Yang et al., 2000; Zaarour et al., 2011). After quenching for 20 min as described above, cells were warmed up to 37°C for 30 or 60 min to permit protein trafficking. Cells were then surface labelled with 1.5 mg/ml sulfo-NHS–biotin and lysed. Lysates were sonicated for 15 s, incubated at 37°C for 20 min and unsolubilised material was pelleted at 13,000*g* for 30 min. The biotinylated fraction, which represents newly inserted surface proteins, was precipitated with streptavidin beads suspension under rotation at 4°C overnight. Beads were washed and biotinylated proteins were extracted in Laemmli buffer with 100 mM DTT, heated at 95°C for 10 min and resolved on gradient 4–15% SDS-PAGE. After transfer, Immobilon P membrane was probed with T4 antibody (1:1000).

Author contribution

M. C. designed the experiments, developed the experimental work, performed data analyses and wrote the paper; F. R. conducted the antibody shift assays, endocytosis–exocytosis assays and silencing experiments; G. P. conducted microscopy confocal analysis; L. Z. and A. M. T. conducted the mass spectometry analysis; D. B. contributed to the design of the antibody shift assay; C. B. and S. T. contributed to the transfection and Western blotting experiments; M. S. supervised the study, was involved in the analysis of the results and supervised the writing of the article.

Funding

This work was supported by the Italian grant PRIN 20078ZZMZW (to M.S.) and by Fondo per gli Investimenti della Ricerca di Base-Rete Nazionale di Proteomica (RBRN07BMCT_009).

Conflict of interest

The authors have declared no conflict of interest.

References

Acuna, R., Martinez-de-la-Maza, L., Ponce-Coria, J., Vazquez, N., Ortal-Vite, P., Pacheco-Alvarez, D., Bobadilla, N.A. and Gamba, G. (2011) Rare mutations in SLC12A1 and SLC12A3 protect against hypertension by reducing the activity of renal salt cotransporters. J. Hypertens. **29**, 475–483

Alvarez-Guerra, M. and Garay, R.P. (2002) Renal Na–K–Cl cotransporter NKCC2 in Dahl salt-sensitive rats. J. Hypertens. **20**, 721–727

Amieva, M.R., Litman, P., Huang, L., Ichimaru, E. and Furthmayr, H. (1999) Disruption of dynamic cell surface architecture of NIH3T3 fibroblasts by the N-terminal domains of moesin and ezrin: *in vivo* imaging with GFP fusion proteins. J. Cell Sci. **112**, 111–125

Ares, G.R. and Ortiz, P.A. (2010) Constitutive endocytosis and recycling of NKCC2 in rat thick ascending limbs. Am. J. Physiol. Renal Physiol. **299**, F1193–1202

Basco, D., Nicchia, G.P., D'Alessandro, A., Zolla, L., Svelto, M. and Frigeri, A. (2011) Absence of aquaporin-4 in skeletal muscle alters proteins involved in bioenergetic pathways and calcium handling. PLoS One **6**, e19225

Basco, D., Nicchia, G.P., Desaphy, J.F., Camerino, D.C., Frigeri, A. and Svelto, M. (2010) Analysis by two-dimensional Blue Native/SDS-PAGE of membrane protein alterations in rat soleus muscle after hindlimb unloading. Eur. J. Appl. Physiol. **110**, 1215–1224

Benziane, B., Demaretz, S., Defontaine, N., Zaarour, N., Cheval, L., Bourgeois, S., Klein, C., Froissart, M., Blanchard, A., Paillard, M., Gamba, G., Houillier, P. and Laghmani, K. (2007) NKCC2 surface expression in mammalian cells: down-regulation by novel interaction with aldolase B. J. Biol. Chem. **282**, 33817–33830

Bretscher, A., Edwards, K. and Fehon, R.G. (2002) ERM proteins and merlin: integrators at the cell cortex. Nat. Rev. Mol. Cell Biol. **3**, 586–599

Caceres, P.S., Ares, G.R. and Ortiz, P.A. (2009) cAMP stimulates apical exocytosis of the renal Na(+)-K(+)-2Cl(-) cotransporter NKCC2 in the thick ascending limb: role of protein kinase A. J. Biol. Chem. **284**, 24965–24971

Camacho-Carvajal, M.M., Wollscheid, B., Aebersold, R., Steimle, V. and Schamel, W.W. (2004) Two-dimensional blue native/SDS gel electrophoresis of multi-protein complexes from whole cellular lysates: a proteomics approach. Mol. Cell. Proteomics **3**, 176–182

Carmosino, M., Gimenez, I., Caplan, M. and Forbush, B. (2008) Exon loss accounts for differential sorting of Na–K–Cl cotransporters in polarized epithelial cells. Mol. Biol. Cell **19**, 4341–4351

Carmosino, M., Rizzo, F., Ferrari, P., Torielli, L., Ferrandi, M., Bianchi, G., Svelto, M. and Valenti, G. (2011) NKCC2 is activated in Milan hypertensive rats contributing to the maintenance of salt-sensitive hypertension. Pflugers Arch. **462**, 281–291

Carmosino, M., Rizzo, F., Procino, G., Basco, D., Valenti, G., Forbush, B., Schaeren-Wiemers, N., Caplan, M.J. and Svelto, M. (2010) MAL/VIP17, a new player in the regulation of NKCC2 in the kidney. Mol. Biol. Cell **21**, 3985–3997

Cha, B., Tse, M., Yun, C., Kovbasnjuk, O., Mohan, S., Hubbard, A., Arpin, M. and Donowitz, M. (2006) The NHE3 juxtamembrane cytoplasmic domain directly binds ezrin: dual role in NHE3 trafficking and mobility in the brush border. Mol. Biol. Cell **17**, 2661–2673

Darman, R.B. and Forbush, B. (2002) A regulatory locus of phosphorylation in the N terminus of the Na–K–Cl cotransporter, NKCC1. J. Biol. Chem. **277**, 37542–37550

Dihazi, H., Asif, A.R., Agarwal, N.K., Doncheva, Y. and Muller, G.A. (2005) Proteomic analysis of cellular response to osmotic stress in thick ascending limb of Henle's loop (TALH) cells. Mol. Cell. Proteomics **4**, 1445–1458

Gamba, G. (1999) Molecular biology of distal nephron sodium transport mechanisms. Kidney Int. **56**, 1606–1622

Gary, R. and Bretscher, A. (1995) Ezrin self-association involves binding of an N-terminal domain to a normally masked C-terminal domain that includes the F-actin binding site. Mol. Biol. Cell **6**, 1061–1075

Gimenez, I. and Forbush, B. (2003) Short-term stimulation of the renal Na–K–Cl cotransporter (NKCC2) by vasopressin involves

UNCORRECTED PROOF

boc-sgml.cls (2004/08/18 v1.0 LaTeX document class BOC) boc201100074.xml June 28, 2012 21:57

phosphorylation and membrane translocation of the protein. J. Biol. Chem. **278**, 26946–26951

Haque, M.Z., Ares, G.R., Caceres, P.S. and Ortiz, P.A. (2011) High salt differentially regulates surface NKCC2 expression in thick ascending limbs of Dahl salt-sensitive and salt-resistant rats. Am. J. Physiol. Renal Physiol. **300**, F1096–F1104

He, X., Tse, C.M., Donowitz, M., Alper, S.L., Gabriel, S.E. and Baum, B.J. (1997) Polarized distribution of key membrane transport proteins in the rat submandibular gland. Pflugers Arch. **433**, 260–268

Hugo, C., Pichler, R., Gordon, K., Schmidt, R., Amieva, M., Couser, W.G., Furthmayr, H. and Johnson, R.J. (1996) The cytoskeletal linking proteins, moesin and radixin, are upregulated by platelet-derived growth factor, but not basic fibroblast growth factor in experimental mesangial proliferative glomerulonephritis. J. Clin. Invest. **97**, 2499–2508

Ishida, N., Hirai, S.I. and Mita, S. (1997) Immunolocalization of aquaporin homologs in mouse lacrimal glands. Biochem. Biophys. Res. Commun.**238**, 891–895

Ji, W., Foo, J.N., O'Roak, B.J., Zhao, H., Larson, M.G., Simon, D.B., Newton-Cheh, C., State, M.W., Levy, D. and Lifton, R.P. (2008) Rare independent mutations in renal salt handling genes contribute to blood pressure variation. Nat. Genet. **40**, 592–599

Kraemer, D.M., Strizek, B., Meyer, H.E., Marcus, K. and Drenckhahn, D. (2003) Kidney Na+,K(+)-ATPase is associated with moesin. Eur. J. Cell Biol. **82**, 87–92

Levi, M. (2003) Role of PDZ domain-containing proteins and ERM proteins in regulation of renal function and dysfunction. J. Am. Soc. Nephrol. **14**, 1949–1951

Liedtke, C.M., Yun, C.H., Kyle, N. and Wang, D. (2002) Protein kinase C epsilon-dependent regulation of cystic fibrosis transmembrane regulator involves binding to a receptor for activated C kinase (RACK1) and RACK1 binding to Na+/H +exchange regulatory factor. J. Biol. Chem. **277**, 22925–22933

Liu, K., Qian, L., Wang, J., Li, W., Deng, X., Chen, X., Sun, W., Wei, H., Qian, X., Jiang, Y. and He, F. (2009) Two-dimensional blue native/SDS-PAGE analysis reveals heat shock protein chaperone machinery involved in hepatitis B virus production in HepG2.2.15 cells. Mol. Cell. Proteomics **8**, 495–505

Mhatre, A.N., Steinbach, S., Hribar, K., Hoque, A.T. and Lalwani, A.K. (1999) Identification of aquaporin 5 (AQP5) within the cochlea: cDNA cloning and *in situ* localization. Biochem. Biophys. Res. Commun. **264**, 157–162

Monette, M.Y., Rinehart, J., Lifton, R.P. and Forbush, B. (2011) Rare mutations in the human Na–K–Cl cotransporter (NKCC2) associated with lower blood pressure exhibit impaired processing and transport function. Am. J. Physiol. Renal Physiol. **300**, F840–F847

Mount, D.B. (2006) Membrane trafficking and the regulation of NKCC2. Am. J. Physiol. Renal Physiol. **290**, F606–F607

Murer, H., Hernando, N., Forster, I. and Biber, J. (2003) Regulation of Na/Pi transporter in the proximal tubule. Annu. Rev. Physiol. **65**, 531–542

Nielsen, S., King, L.S., Christensen, B.M. and Agre, P. (1997) Aquaporins in complex tissues. II. Subcellular distribution in respiratory and glandular tissues of rat. Am. J. Physiol. **273**, C1549–C1561

Ortiz, P.A. (2006) cAMP increases surface expression of NKCC2 in rat thick ascending limbs: role of VAMP. Am. J. Physiol. Renal Physiol. **290**, F608–F616

Pyndiah, S., Lasserre, J.P., Menard, A., Claverol, S., Prouzet-Mauleon, V., Megraud, F., Zerbib, F. and Bonneu, M. (2007) Two-dimensional blue native/SDS gel electrophoresis of multiprotein complexes from Helicobacter pylori. Mol. Cell. Proteomics **6**, 193–206

Russell, J.M. (2000) Sodium–potassium–chloride cotransport. Physiol. Rev. **80**, 211–276

Schagger, H. and von Jagow, G. (1991) Blue native electrophoresis for isolation of membrane protein complexes in enzymatically active form. Anal. Biochem. **199**, 223–231

Shenolikar, S. and Weinman, E.J. (2001) NHERF: targeting and trafficking membrane proteins. Am. J. Physiol. Renal Physiol. **280**, F389–F395

Short, D.B., Trotter, K.W., Reczek, D., Kreda, S.M., Bretscher, A., Boucher, R.C., Stutts, M.J. and Milgram, S.L. (1998) An apical PDZ protein anchors the cystic fibrosis transmembrane conductance regulator to the cytoskeleton. J. Biol. Chem. **273**, 19797–19801

Simon, D.B., Karet, F.E., Hamdan, J.M., DiPietro, A., Sanjad, S.A. and Lifton, R.P. (1996) Bartter's syndrome, hypokalaemic alkalosis with hypercalciuria, is caused by mutations in the Na-K-2Cl cotransporter NKCC2. Nat. Genet. **13**, 183–188

Sonalker, P.A., Tofovic, S.P. and Jackson, E.K. (2004) Increased expression of the sodium transporter BSC-1 in spontaneously hypertensive rats. J. Pharmacol. Exp. Ther. **311**, 1052–1061

Sonalker, P.A., Tofovic, S.P. and Jackson, E.K. (2007) Cellular distribution of the renal bumetanide-sensitive Na-K-2Cl cotransporter BSC-1 in the inner stripe of the outer medulla during the development of hypertension in the spontaneously hypertensive rat. Clin. Exp. Pharmacol. Physiol. **34**, 1307–1312

Stanasila, L., Abuin, L., Diviani, D. and Cotecchia, S. (2006) Ezrin directly interacts with the alpha1b-adrenergic receptor and plays a role in receptor recycling. J. Biol. Chem. **281**, 4354–4363

Starremans, P.G., Kersten, F.F., Knoers, N.V., van den Heuvel, L.P. and Bindels, R.J. (2003) Mutations in the human Na–K–2Cl cotransporter (NKCC2) identified in Bartter syndrome type I consistently result in nonfunctional transporters. J. Am. Soc. Nephrol. **14**, 1419–1426

Sun, F., Hug, M.J., Bradbury, N.A. and Frizzell, R.A. (2000) Protein kinase A associates with cystic fibrosis transmembrane conductance regulator via an interaction with ezrin. J. Biol. Chem. **275**, 14360–14366

Swiatecka-Urban, A., Duhaime, M., Coutermarsh, B., Karlson, K.H., Collawn, J., Milewski, M., Cutting, G.R., Guggino, W.B., Langford, G. and Stanton, B.A. (2002) PDZ domain interaction controls the endocytic recycling of the cystic fibrosis transmembrane conductance regulator. J. Biol. Chem. **277**, 40099–40105

Uawithya, P., Pisitkun, T., Ruttenberg, B.E. and Knepper, M.A. (2008) Transcriptional profiling of native inner medullary collecting duct cells from rat kidney. Physiol. Genomics **32**, 229–253

Wang, S., Yue, H., Derin, R.B., Guggino, W.B. and Li, M. (2000) Accessory protein facilitated CFTR–CFTR interaction, a molecular mechanism to potentiate the chloride channel activity. Cell **103**, 169–179

Wellner, R.B. and Baum, B.J. (2001) Polarized sorting of aquaporins 5 and 8 in stable MDCK-II transfectants. Biochem. Biophys. Res. Commun. **285**, 1253–1258

Yang, X., Amemiya, M., Peng, Y., Moe, O.W., Preisig, P.A. and Alpern, R.J. (2000) Acid incubation causes exocytic insertion of NHE3 in OKP cells. Am. J. Physiol. Cell Physiol. **279**, C410–C419

Zaarour, N., Defontaine, N., Demaretz, S., Azroyan, A., Cheval, L. and Laghmani, K. (2011) Secretory carrier membrane protein 2 regulates exocytic insertion of NKCC2 into the cell membrane. J. Biol. Chem. **286**, 9489–9502

Received: 24 December 2011; Accepted: 15 June 2012; Accepted article online: DD MM YYYY

UNCORRECTED PROOF

Biology of the Cell

WILEY-BLACKWELL

Manuscript No.: boc201100074

Please correct your galley proofs and return them within 48h of receipt.
Note: The editors reserve the right to publish your article without your corrections if the proofs do not arrive in time.

Important

Please note that, due to the size constraints of emailed attachments, the attached proofs are low resolution; however, please be assured that high resolution versions will be used for printing.

Check the galley proofs very carefully, paying particular attention to the formulae, figures, numerical values, and tabulated data. An author query (AQ) in the border indicates unclear or missing information that requires **your attention**. For the complete query, please consult the attached list. Note that the author is liable for damages arising from incorrect statements, including misprints.

Your corrections should be provided as a list (*e.g.* in Word format), including the page number, column, section number and line at which the correction occurs. In addition, we ask that you provide a scanned pdf of the proof with corrections, if possible, to reduce the risk of errors.

Please return your corrections by email to the following address:

E-Mail: blackwelluk@aptaracorp.com
If you have any comments, however minor, on the handling of the paper, please let us know. Please quote the paper's reference number (DOI) when doing so.

Please limit corrections to printing errors; costs incurred for any further changes or additions will be charged to the author, unless such changes have been accepted by the editor.

If you have any queries, please contact the BOC Managing Editor:

BOCManagingEditor@wiley.com

UNCORRECTED PROOF

QUERY FORM

Wiley-Blackwell

JOURNAL TITLE: BOC 6/28/2012
ARTICLE NO: boc201100074

Queries and / or remarks

Query No.	Details Required	Author's Response
Q1	Please replace GFP with its full form in the Abstract and define GFP at its first occurrence in the text.	
Q2	Please check the equal contribution footnote for correctness.	
Q3	'Recently, it … (Haque et al., 2011)'. The meaning of this sentence is not clear; please rewrite or confirm that the sentence is correct.	
Q4	'Similar to …. Wellner and Baum, 2011'. The meaning of this sentence is not clear; please rewrite or confirm that the sentence is correct.	
Q5	'Interestingly, we … (Figure 5B, AQP5, red)'. This sentence has been edited for clarity. Please check and confirm it is correct.	
Q6	Please replace 'Figure C' in the sentence 'Densitometric analysis NKCC2 phosphorylation' with a specific figure number.	
Q7	Please define CFTR at its first occurrence.	
Q8	Please replace PKA with its full form.	
Q9	Please replace RP, HPLC and ESI with their respective full forms.	
Q10	Please define DTt at its first occurrence.	
Q11	Please define EBS at its first occurrence.	
Q12	Please replace PMSF with its full form.	

Q1. Replace GFP with Green Fluorescent Protein.

Q2. OK

Q3. OK

Q4. OK

Q5. Remove 'anti-' from anti-acquaporin 5

Q6. Change Figure C with Figure 6C

Q7. Define CFTR as Cystic fibrosis transmembrane conductance regulator

Q8. Replace PKA with Protein kinase A

Q9. Define RP-HPLC-ESI as Reverse Phase (RP) High Performance Liquid Chromatography (HPLC) Electrospray Ionization (ESI)

Q10. Define DTT as Dithiothreitol

Q11. Define EBS as Earle's Balanced Salts

Q12. Replace PMSF with the full name Phenyl Methyl Sulfonyl Fluoride.

UNCORRECTED PROOF

The most important correction marks

Typesetting error	Correction mark in the text	Correction mark in the right-hand margin
Wrong letter, wrong word	Metal tyke was the ~~try~~ to	~~p~~ H key
Missing letter(s)	the ivention of prin,	~~nv~~ ting
Missing word	and assembly into printed page	its the
Wrong word division, missing punctuation mark	was the only step a prin- ter could take until recently	nt ~~g~~ ((2x)) ,
Defect letter, soiled text (in case of illegibility to be treated as a wrong letter or word)	towards obtaining a surface from which impressions can	
Letters/words to be deleted	be made. Printing ~~of~~ from	~~g~~ H~~g~~
Letters in wrong sequence	movable type stated	~~le~~ ar
Two words in wrong sequence	1440 around Since	
Several words in wrong sequence	in this of printing account typefounding place has no	1-9
Wrong space, missing space	we may dispense with an account of how type	((2x))
Space between words too large or too small	comes into being and start with the type itself.	((2x))
Characters not on a straight line	Initially we may concentrate	
Space between lines too narrow	on a single process – letterpress – because metal type was once the	
Space between lines too wide	only printing surface available to that process.	
Wrong typeface	A historical view of printing would *have* to take into account a period in which type casting	((italics)) ((normal typeface)) w
Start new paragraph	and type-setting remained unchanged. But type has	
Undesired new paragraph	continuously consolidated and extended	
Undesired indentation	the domain of the printed word. The most important changes came with:	
Missing indentation	automatic composing,	
Blockade	^{1}H-NMR (-MHz)	/ 300